



Sound radiation from the waveguide double plate regarding air cavity between the upper and lower plates

H. KIM ; J. RYUE¹

¹ School of Naval Architecture and Ocean Engineering, University of Ulsan, Korea

ABSTRACT

In this study, the vibration and sound radiation from the double-layered strip plate with air cavity between the upper and lower plates are investigated by using the waveguide finite and boundary element method. The interaction between the structural and acoustic waves propagating along the double-layered strip plate is investigated by observing the dispersion relations of the waves. The vibration and sound radiation from the double-layered strip plate with and without the air cavity are compared. From this study, the interaction between the structural and acoustic waves appear in the dispersion curves due to the air cavity. The large variations of the vibration and radiated power between the unstiffened and stiffened double plates are observed due to the air cavity. As the stiffeners are added, however, its contribution becomes less.

Keywords: Air cavity, Double-layered strip plate, Radiation efficiency, Waveguide finite element /boundary element method, I-INCE Classification of Subjects Number(s): 23.1, 42

1. INTRODUCTION

Many large structures like ships, trains, etc. are often built with stiffened double layered plates. To be able to predict the vibrational response and sound radiation of these structures, it is necessary to understand the fundamental vibrating and radiating behaviors of these double layered plates.

The vibration and sound radiation for stiffened double layered strip plates were investigated disregarding the air cavities between the upper and lower plates in ref. [1]. However, the air cavities are coupled with the upper and lower plates so that they must contribute to the response of the double layered plates. In this paper, vibration characteristics and sound radiations of infinite length strip double layered plates with air cavities are investigated numerically by means of the waveguide finite element and boundary element (WFE/BE) method[1-7]. In this numerical analysis, single and three longitudinal stiffeners are modeled between the upper and lower plates of double plate to examine the effects of air cavities on the wave propagation and sound radiation.

Above all, the dispersion diagrams are obtained to observe the features of structural waves and the interaction between the structural and acoustic waves propagated along the double layered strip plate. The forced responses for the plates are also evaluated by calculating average mean-squared velocities of the lower plate(radiating plate) when a point force is applied on the upper plate. In terms of sound radiation, sound powers radiated from the lower plate are calculated and then the radiation efficiencies are presented. Finally, the vibration and sound radiation from the double-layered strip plate with and without the air cavities are compared to examine effects of the air cavities.

2. THE WAVEGUIDE FINITE ELEMENT AND BOUNDARY ELEMENT ANALYSIS

In this paper, a numerical method called waveguide finite element and boundary element method is applied to the double layered strip plate. The WFE method models only 2D cross-sections of the waveguide structures but takes into account the 3D nature of the infinite extent of the waveguide. If the WFE model is contacted with fluids, fluids existing inside and outside of waveguide structure can be modeled by FEs and BEs, respectively. This coupled WFE/BE method can be adopted to investigate sound radiations from the waveguide structures connected to the fluid. The WFE/BE method is briefly described here and details for this method refer to refs[1-7].

¹ jsryue@ulsan.ac.kr

The WFE equation for the waveguide structure with plate elements is given by

$$\{\mathbf{K}_{s4}(-i\kappa)^4 + \mathbf{K}_{s2}(-i\kappa)^2 + \mathbf{K}_{s1}(-i\kappa) + \mathbf{K}_{s0} - \omega^2 \mathbf{M}_s\} \tilde{\Phi} = \tilde{\mathbf{F}}_s, \quad (1)$$

where \mathbf{K}_{s4} , \mathbf{K}_{s2} , \mathbf{K}_{s1} and \mathbf{K}_{s0} are the matrices that come from the stiffness of the structure, \mathbf{M}_s is the mass matrix, κ is the structural wavenumber in the x direction, $\tilde{\Phi}$ is the displacement vector representing shapes of cross-sectional deformation, and $\tilde{\mathbf{F}}_s$ is the vector of excitation forces.

In case that inside of waveguide structures is filled with a fluid, it can be considered by modeling the fluid with WFEs. The WFE equation for the fluid is given by

$$\{\mathbf{K}_{f2}(-i\kappa)^2 + \mathbf{K}_{f0} - \omega^2 \mathbf{M}_f\} \tilde{\Psi}_m = \tilde{\mathbf{F}}_f, \quad (2)$$

the subscript f denotes the fluid part. \mathbf{K}_{f2} and \mathbf{K}_{f0} are the stiffness matrices, \mathbf{M}_f is the mass matrix, $\tilde{\Psi}_m$ is the velocity potential of the fluid inside, $\tilde{\mathbf{F}}_f$ is the external force applied to the fluid. The right-hand side of Eq. (2) sets to zero, in this study, because there is no excitation force to the fluid.

The inside fluid and waveguide structure are coupled, hence the governing equation is given by

$$\left[\begin{array}{cc} \mathbf{K}_s & \mathbf{0} \\ \mathbf{0} & \mathbf{K}_f \end{array} \right] + i\omega \left[\begin{array}{cc} \mathbf{0} & \mathbf{C}_3 \\ -\mathbf{C}_3^T & \mathbf{0} \end{array} \right] - \omega \left[\begin{array}{cc} \mathbf{M}_s & \mathbf{0} \\ \mathbf{0} & \mathbf{M}_f \end{array} \right] \left\{ \begin{array}{c} \tilde{\Phi} \\ \tilde{\Psi}_m \end{array} \right\} = \left\{ \begin{array}{c} \tilde{\mathbf{F}}_s \\ \mathbf{0} \end{array} \right\}, \quad (3)$$

where $\mathbf{K}_s = \mathbf{K}_{s4}(-i\kappa)^4 + \mathbf{K}_{s2}(-i\kappa)^2 + \mathbf{K}_{s1}(-i\kappa) + \mathbf{K}_{s0}$, $\mathbf{K}_f = \mathbf{K}_{f2}(-i\kappa)^2 + \mathbf{K}_{f0}$ and \mathbf{C}_3 is the coupled matrix between the waveguide structure and internal fluid.

For waveguide structures coupled with exterior fluid, the boundary elements are introduced, and connected with the WFEs. The equation for the WFE model coupled with the BEs is written by

$$\{\mathbf{K}_s - \omega^2 \mathbf{M}_s\} \tilde{\Phi} + i\omega \mathbf{C}_3 \tilde{\Psi}_m = \tilde{\mathbf{F}}_s + i\omega \rho \mathbf{C}_1 \tilde{\Psi}_{ex}, \quad (4)$$

where \mathbf{C}_1 is the coupled matrix between the WFEs and BEs, and $\tilde{\Psi}_{ex}$ denotes the velocity potential vector defined at the nodes of the BEs. If a fluid contacted to the WFE model is light like air, the second term of the right-hand side in Eq. (4) can be disregarded. Hence $\tilde{\Phi}$ in Eq. (4) can be obtained by substituting $\tilde{\Psi}_m$ in Eq. (3) as a function of $\tilde{\Phi}$.

The continuity condition at the coupled dofs between the structure and external fluid is given by

$$i\omega \mathbf{C}_2 \tilde{\Phi} - \mathbf{I}_2 \frac{\partial \tilde{\Psi}_{ex}}{\partial \mathbf{n}} = \mathbf{0}, \quad (5)$$

where \mathbf{n} is a normal directional vector of the BEs connected with the WFEs, \mathbf{I}_2 is an identity matrix and \mathbf{C}_2 is a matrix allocating dofs fluid coupled in $\tilde{\Phi}$. In case of air, $\partial \tilde{\Psi}_{ex} / \partial \mathbf{n}$ can be calculated from the coupling condition between the WFEs and BEs in Eq. (5) by substituting $\tilde{\Phi}$ obtained from Eq. (4).

The velocity potential, $\tilde{\Psi}_{ex}$, and the normal velocity, $\partial \tilde{\Psi}_{ex} / \partial \mathbf{n}$, at the coupled boundary can be found by

$$\mathbf{H} \tilde{\Psi}_{ex} - \mathbf{G} \frac{\partial \tilde{\Psi}_{ex}}{\partial \mathbf{n}} = \mathbf{0}, \quad (6)$$

where \mathbf{H} and \mathbf{G} are matrices of Green's function. By solving Eqs (5)~(6), sound pressure $\tilde{p}(\kappa)$ and normal directional particle velocity $\tilde{v}(\kappa)$ at the coupled boundary are determined.

3. APPLICATION OF THE WFE AND BE METHOD TO THE DOUBLE LAYERED PLATE WITH AND WITHOUT AIR CAVITY

In this section, the WFE/BE method is applied to the unstiffened and stiffened double layered plates with and without air cavity to examine the effects of air cavity between the upper and lower plates. The

Table 1 – Dimensions and material properties of the upper and lower plates

Young’s modulus, E	71GPa
Poisson’s ratio, ν	0.332
Thickness, h	6mm
Width, l_y	1m
Density, ρ	2700kg/m ³
Damping loss factor, η	0.01

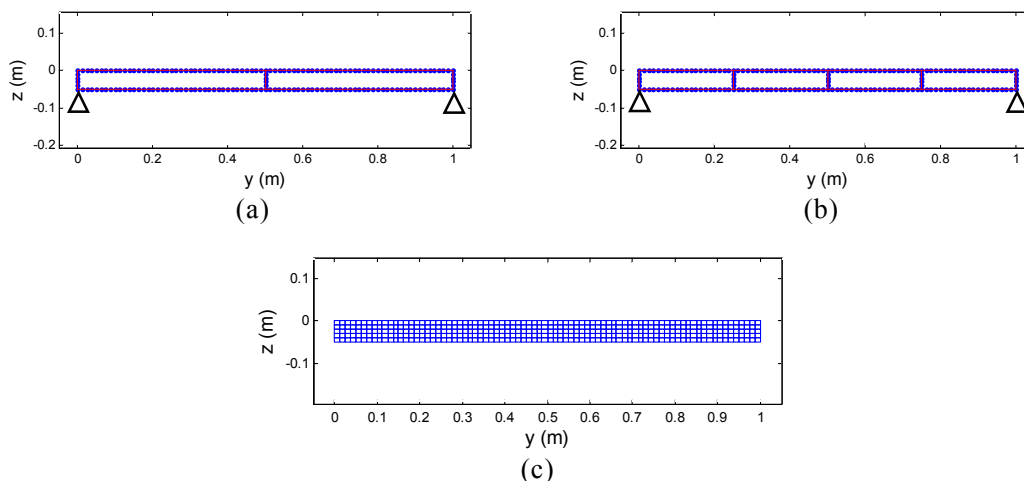


Figure 1 – Cross-sectional models of a double plate, with (a) a single and (b) three stiffeners, and (c) a fluid

cross-sectional models for the stiffened double layered plates are shown in Figure 1. These models have infinite lengths along the x direction. The properties and dimensions of the upper and lower plates are listed in Table 1. The lower plates are simply supported at both ends. The thickness and height of the stiffeners are set to 6 mm and 5 cm, respectively. A point force is set to apply on the upper plates at $y = 0.425$ m in the vertical direction. In this WFE analysis, the unstiffened double plate is also examined to compare the results with those of stiffened plates to evaluate the effects of the stiffeners.

The internal fluid between the top and bottom plate can be modeled with FEs. The FE model for the internal air between the upper and lower plates is shown in Figure 1(c) with 80×5 elements. The number of stiffeners were chosen to one and three as shown in Figure 1(a) and (b). For the model with a single stiffener in the middle, the width of the air cavity becomes 50 cm and then two bays are formed in each plate. Similarly, the model with three stiffeners has four air cavities and four bays in the upper and lower plates each.

For the calculation of radiated sound, the BEs which have the same topology as the FEs of the lower plate are coupled on the bottom side of the lower plate. Baffled boundary condition is allocated to the region of $y < 0$ and $y > l_y$ at $z = 0$.

3.1 Dispersion Relation

Prior to the dispersion curves of the structure coupled with a fluid between the upper and lower plates, it is necessary to understand dispersion relation of the fluid. The dispersion curves of the fluid between the upper and lower plates unstiffened are shown in Figure 2. To observe characteristics of the acoustic waves propagating through the cavity, the pressure distributions marked with ‘+’ and ‘×’ in Figure 2 are shown in Figure 3. There are lots of dispersion curves concentrated on high frequency range as shown in Figure 2. That is because of acoustic waves which has modes in the z direction.

For the unstiffened double plate, the dispersion curves are illustrated in Figure 4. It is shown in Figure 4 that two dispersion curves are paired off. One in each pair has anti-phase deformation between the upper and lower plates and the others does in-phase. It is seen in Figure 4(a) that the

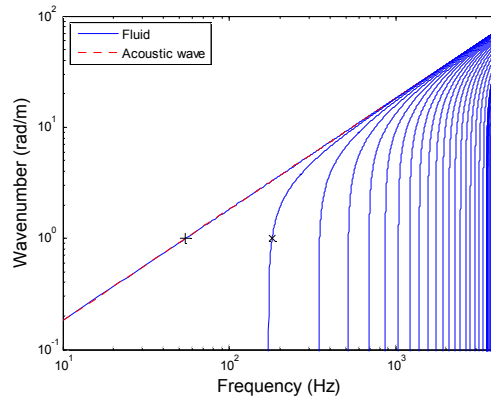


Figure 2 – Dispersion diagram of the fluid between the upper and lower plate

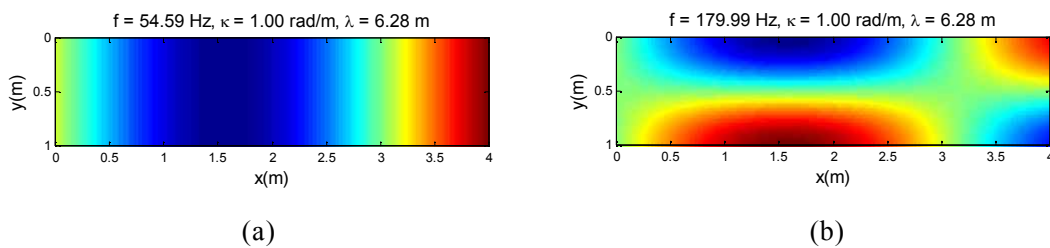


Figure 3 – The pressure distributions marked with (a) ‘+’ and (b) ‘x’ in Figure 2

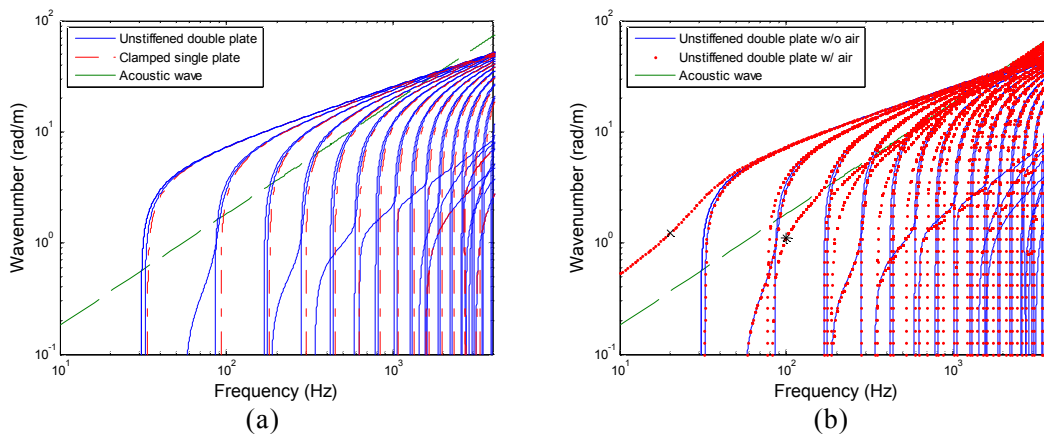


Figure 4 – Dispersion diagram of the unstiffened double plate (a) without and (b) with air cavity

dispersion curves of the unstiffened double plate are approximated by those of a single plate with clamped boundaries at both ends. This is due to the side plates at $y = 0$ and $y = l_y$, working like rigid walls.

The dispersion curves of the unstiffened double plate with an air cavity are also shown in Figure 4(b). It can be found from Figure 4(b) that the structural and acoustic waves are strongly coupled. For example, the first structural and acoustic waves in Figure 4(a) are strongly coupled together so that the first coupled wave in Figure 4(b) at low frequency has larger wavenumber than that of the uncoupled acoustic wave. To observe the characteristics of these two waves, the deformation shapes marked with ‘x’ and ‘*’ in Figure 4(b) are shown in Figure 6(a). It can be expected from Figure 6(a) that these waves largely contribute to the vibration of the double plate.

The dispersion curves obtained from the double plate with a single stiffener is shown in Figure 5. It is seen from Figure 5 that four waves come close and grouped as the wavenumber increases. The mode shapes of the waves in the first group marked with ‘*’ in Figure 5(a) are shown in Figure 6(b) in order. It can be thought from Figure 6(b) that the single stiffener rarely contributes to the deformation of the first wave in low wavenumber region as shown in Figure 6(b). As the frequency increase, on the contrary, the stiffener plays like a rigid wall and the dispersion curves are approximated to those of the clamped half plate as compared in Figure 5(a). In addition, it is expected that the mode shapes of the

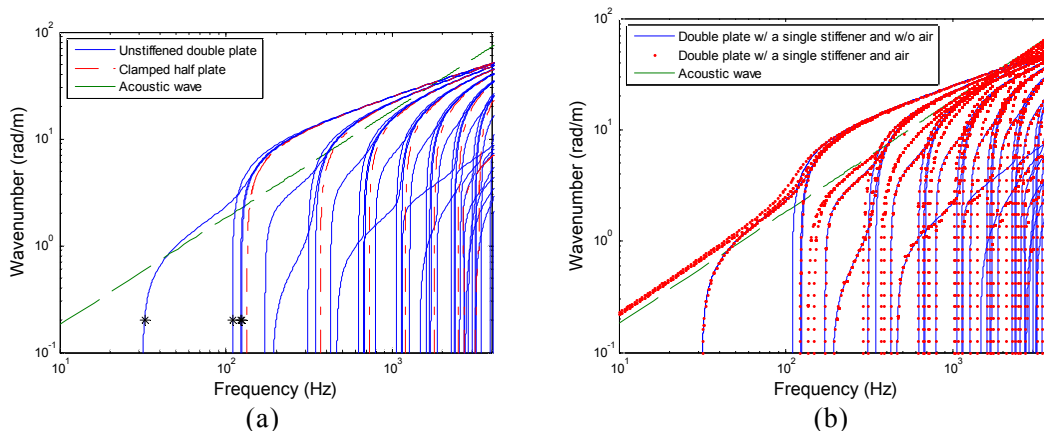


Figure 5 – Dispersion diagram of the double plate with a single plate (a) without and (b) with air cavity

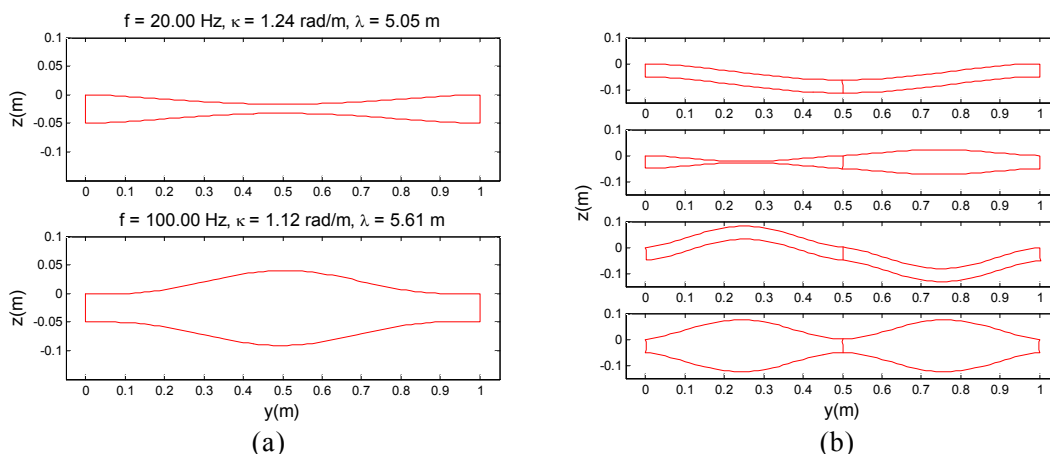


Figure 6 – The deformation shapes (a) marked with ‘×’ and ‘*’ in Figure 4(b) at 20 and 100Hz (b) marked with ‘*’ in Figure 5(a)

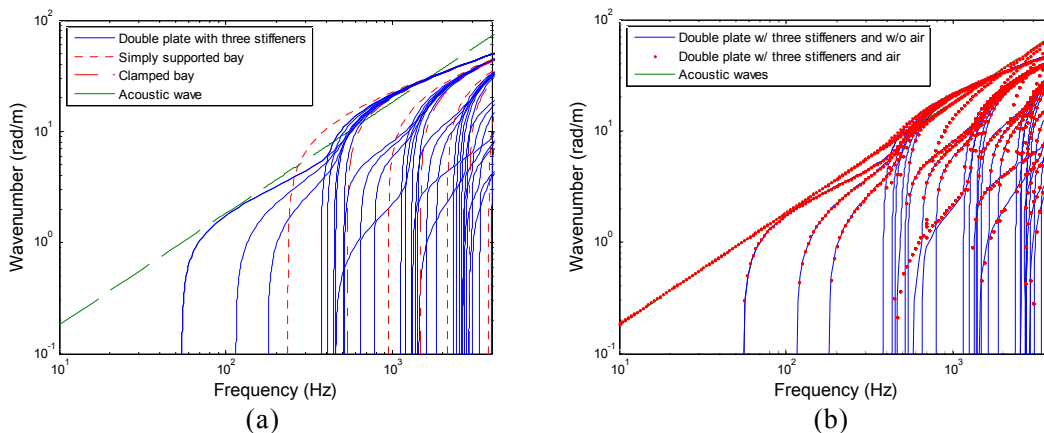


Figure 7 – Dispersion diagram of the double plate with three stiffeners (a) without and (b) with air cavity

the second and fourth waves in Figure 6(b) interacts effectively with air cavities.

The dispersion curves of the double plate with a single stiffener with air cavity is illustrated in Figure 5(b). Figure 5(b) shows that there are additional waves propagating through the two cavities inside the double plate. Since there are two cavities, two acoustic waves are coupled with structural waves in each group in Figure 5(a).

For the double plate with the three stiffeners shown in Figure 1(b), the dispersion curves are illustrated in Figure 7. The similar features of the wave grouping are found in Figure 7. Each group

contains eight waves in general, corresponding to the number of bays in the lower and upper plates. It is seen in Figure 7(a) that eight waves in each group are bounded by those of a single bay with simply supported and clamped boundaries at both ends. The dispersion diagram obtained from the double plate with three stiffeners and internal air is shown in Figure 7(b). It is shown that there are additional waves which propagate through the four air cavities. The coupling between the structural and acoustic waves also appears and four in each group have strong interaction. Compare to the unstiffened and single stiffened plates, the strength of the coupling between the structural and acoustic waves tends to be weakened as the number of stiffeners grows.

3.2 Forced vibration responses

Prior to the stiffened plates, the average mean-squared velocity of the unstiffened double plate is shown in Figure 8(a). It is seen in Figure 8(a) that there are peaks corresponding to the cut-on frequencies as shown in Figure 4(a). To observe the effects of the air cavity on the average mean-squared velocity, the response of the unstiffened double plate with internal air is compared in Figure 8(a). The effects of the air cavity appear predominantly below the first cut-on frequency and a range between about 70 and 200Hz. To see the responses of these two ranges in wavenumber domain, the average mean-squared velocities at 20 and 100Hz are compared in Figure 9(a) with and without the air cavity. It is found in Figure 9(a) that the response increases significantly at the wavenumbers of the plate-air-plate resonances, marked with 'x' and '*' in Figure 4(b).

For the average mean-squared velocity of the double plate with a single stiffener, the response of the lower plate generated from a point force applied on the upper plate are shown in Figure 8(b). Figure 8(b) shows that the plate has large vibrations at frequencies where the many waves are cut-on. With the air cavity between the upper and lower plates, the average mean-squared velocity is also shown in Figure 8(b). The presence of the air cavity introduces a slight change of the vibration mainly above a hundred Hertz but little differences below that. The response of the double plate with a single stiffener is also calculated against the wavenumber at 20Hz and shown in Figure 9(b). The wavenumber domain response is nearly the same as that of none air cavity except around 0.47 rad/m where the effect of the

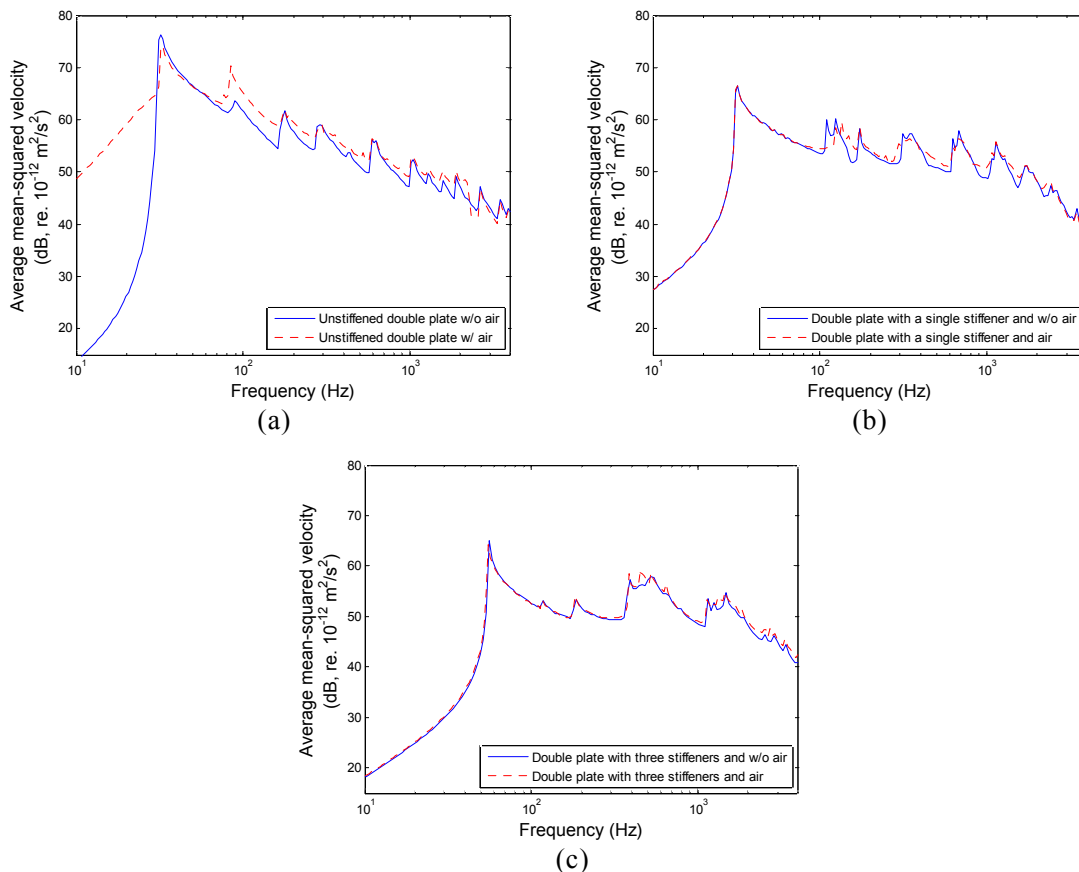


Figure 8 – The average mean-squared velocities of the double plate (a) without stiffeners, (b) with a single stiffener and (c) three stiffeners excited at $y=0.425m$

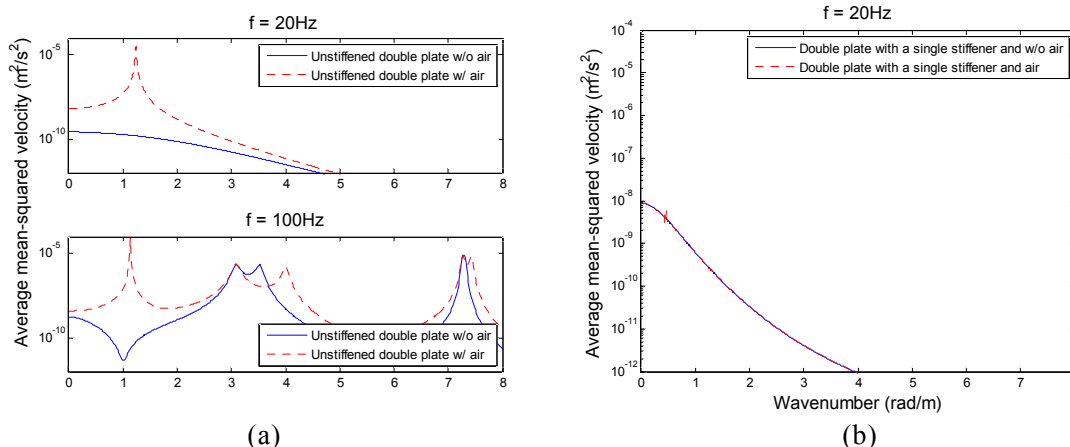


Figure 9 – The average mean-squared velocities of the double plate (a) without stiffeners at 20 and 100Hz, (b) with a single stiffener at 20Hz

air cavity appears as small peaks. From Figure 9(b), it is recognized that the air cavity does not affect much because of the presence of the stiffener at low frequencies.

The response of the double plate with the three stiffeners are shown in Figure 8(c). There are three humps in frequencies between 300Hz and 3kHz as illustrated in Figure 8(c). The humps in this frequency range are associated with the bunch of waves shown in Figure 7 concentrated on these frequencies. Similar to response of the double plate with a single stiffener, the air cavities between the upper and lower plates little contributes to the response of the double plate.

3.3 Radiated sound power

To radiate the sound from the plate, the z directional wavenumber ($k_z = \sqrt{k^2 - k_x^2 - k_y^2}$) should be real. That is,

$$k^2 > k_x^2 + k_y^2, \tag{7}$$

where k , k_x and k_y are the acoustic, the x and y directional wavenumbers. The radiated sound power from the lower plate is shown in Figure 10. Figure 10 shows that at low frequencies the plate radiates the sound dominantly only around the cut-on frequencies at low frequencies because the condition in Eq. (7) is satisfied around the cut-on as shown in Figure 4(a). The sound power of the unstiffened double plate with the air cavity is also illustrated in Figure 10(a). It can be found from Figure 10 that the sound power increases most of the frequencies, especially below 200Hz. The sound powers in wavenumber domain are compared in Figure 11 at 20 and 100Hz regarding the presence of the air cavity. Figure 11 shows that the sound power is generated from the vibration of the plate in wavenumbers smaller than the acoustic wavenumber. The radiated power at 100Hz in Figure 11 shows a peak at 1.12 rad/m, which is not shown in the sound power without the air cavity.

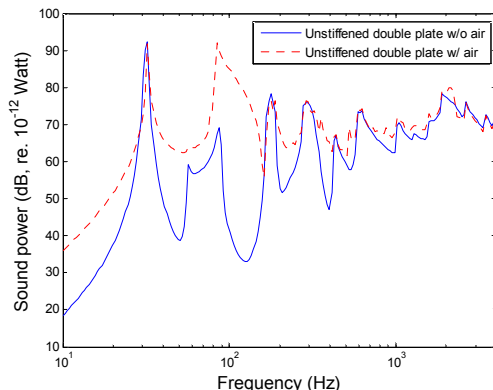


Figure 10 – The radiated powers of unstiffened double plate with and without air cavity excited at $y = 0.425\text{m}$

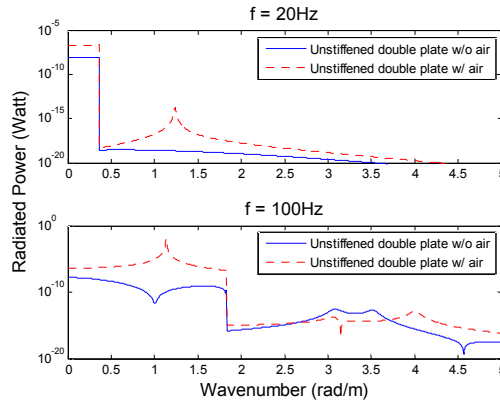


Figure 11 – The radiated powers of unstiffened double plate at 20 and 100Hz

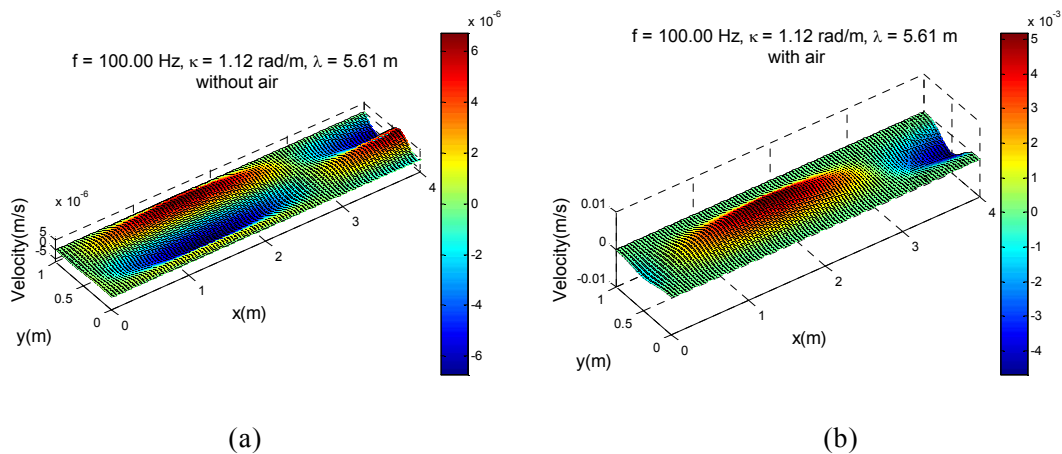


Figure 12 – The velocity of the lower plate of unstiffened double plate (a) without and (b) with air cavity at 100Hz and 1.12 rad/m

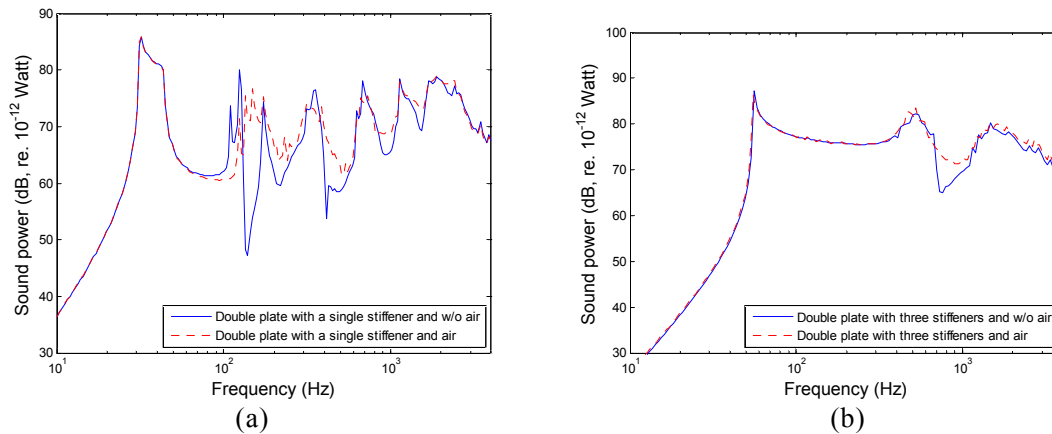


Figure 13 – The radiated powers of the double plates, with (a) a single and (b) three stiffeners, with and without air cavity excited at $y=0.425m$

The velocities of the upper plate without and with the air at this peak are shown in Figure 12(a) and (b), respectively. If there is no air cavity, the lower plate have the second mode in the y direction. However, if there is an air cavity, the lower plate shows the first mode in the y direction. It can be said from this comparison that the air cavity makes the lower plate radiate sound more.

The sound power of the double plate with a single plate is calculated and shown in Figure 13(a). In Figure 13(a), the contribution of the air cavity to the sound power has decreased compare to the unstiffened double plate. The main difference between the sound power with and without the air cavity appears above 100Hz. This variation comes from the effects of the acoustic wave. The sound

powers radiated from the double plate with the three stiffeners are shown in Figure 13(b). The effects of air cavities do not appear much except between 500 and 1000 Hz where the strong coupling appears.

4. Conclusion

In this study, characteristics of wave propagation along the unstiffened and stiffened double strip plates were investigated regarding the contribution of the air cavity. In addition, the sound radiations were explored numerically by using the WFE/BE method. To examine the effects of the air cavities within the double plate, the internal fluid was included with FEs in this analysis.

The wave types were strongly affected by the stiffeners, especially at higher frequencies. Since the stiffeners worked like a rigid boundary at high frequencies, the waves in bays of the plate became an important parameter. The air cavity between the upper and lower plates has induced a considerable variation of dispersion curves of structural waves around coincidence frequencies. As the number of stiffeners increased, however, the strength of coupling between the structural and acoustic waves was weakened.

For the average mean-squared velocity of the unstiffened double plate, the air cavity between the upper and lower plates largely affected in the structural response below the first cut-on frequency. On the contrary, the air cavity hardly contribute to that of the double plate with a single stiffener in this low frequency range. As the stiffeners are added, the effects of the air cavity on the responses above the first cut-on frequency became less.

For the sound power, the presence of the air cavity made the lower plate radiate more. It was found from the sound power of the stiffened double plates that the increment of the sound power was shown in the frequency ranges where the strong coupling appears. However, these frequency ranges decreased increases as the number of the stiffeners increase.

In the present study, the point force was applied to the plate to investigate the effects of stiffeners and air cavity. The sound transmission through unstiffened, stiffened and double plates is going to be investigated by using the same WFE/BE method in further work.

ACKNOWLEDGEMENTS

This research was supported by Basic Science Research Program through the National Research Foundation of Korea(NRF) funded by the Ministry of Education (2012R1A1A1002779).

REFERENCES

1. H. Kim and J. Ryue, Sound radiation from strip plates with longitudinal stiffeners using waveguide finite and boundary element methods, *Journal of Mechanical Science and Technology*, 28(7), 2014, pp. 2527-2534.
2. C. M. Nilsson, Waveguide finite elements applied on a car tyre, Ph. D. thesis, KTH, Stockholm, Sweden, 2004.
3. I. Prasetyo, Investigation of sound transmission in lightweight structures using a waveguide finite element/boundary element approach, Ph. D. thesis, University of Southampton, UK, 2012.
4. J. Ryue, D. J. Thompson, P.R. White and D. R. Thompson, Decay rates of propagating waves in railway tracks at high frequencies, *Journal of Sound and Vibration*, 320, 2009, pp. 955-976.
5. J. Ryue, D. J. Thompson, P.R. White and D. R. Thompson, Investigations of propagating wave types in railway tracks at high frequencies, *Journal of Sound and Vibration*, 315, 2008, pp. 157-175.
6. C. M. Nilsson, C. J. C. Jones, D. J. Thompson and J. Ryue, A waveguide finite element and boundary element approach to calculating the sound radiated by railway and tram rails, *Journal of Sound and Vibration*, 321, 2009, pp. 813-836.
7. U. Orrenius and S. Finnveden, Calculation of wave propagation in rib-stiffened plate structure, *Journal of Sound and Vibration*, 198 (2), 1996, pp. 203-224.